UNIVERSIDAD DE SONORA

FACULTAD INTERDISCIPLINARIA DE CIENCIAS EXACTAS Y NATURALES DEPARTAMENTO DE INVESTIGACIÓN EN FÍSICA

THESIS

in partial fulfillment of the requirements for the degree of:

Maestría en Ciencias (Física)

By:

Julio César Borbón Fragoso

Director:
Dr. Jose Feliciano BENITEZ RUBIO

Hermosillo, Sonora   2025

Table of contents

List of figures

List of tables

Chapter 1

Introduction

1.1 Particle Physics and the Standard Model

Elementary particle physics is the study of the particles at the most fundamental level, the constituents of the universe as well as the interactions between them which are called, electromagnetic force, nuclear weak force and nuclear strong force and there is also the gravity force but this one doesn't have a satisfactory quantum theory for it. Each of these forces are mediated by exchange particles, in the case of the electromagnetic force the mediator is the photon, for the strong force the gluons, for the weak force the bosons W and Z and for the gravity we have the hypothetical graviton. [1]

Force	Strength	Theory	Mediator
Strong	10	Chromodynamics	Gluon
Electromagnetic	10^{-2}	Electrodynamics	Photon
Weak	10^{-13}	Flavordynamics	W and Z
Gravitational	10^{-42}	Geometrodynamics	Graviton

Fig. 1.1 Comparison of the strength magnitude of the four fundamental forces

Each of these forces have a mathematical description for the physical systems of these interactions using the Quantum Field Theory (QFT). The one that describes systems under the electromagnetic force is called Quantum Electrodynamics (QED) this force dictates the electronic structure of atoms being the low energy manifestation of the electromagnetic theory. For the strong force Quantum Chromodynamics (QCD) is the fundamental theory of strong interactions, this force is responsible of maintaining protons and neutrons together

in the atomic nucleus. For the weak interactions there is no particular name in the same way as the previous two, this force is is carried by all quarks and leptons and is responsible for the β Decay of some radioactive isotopes and nuclear processes of the sun. [2]

Almost all the physical phenomena can be explained with only the electron, the electron neutrino, the proton and the neutron interacting with the electromagnetic force, the strong force and the weak one. When higher levels of energy are present new particles are observed, all of this is known as the elementary particles which are embodied in the standard model of particle physics that is by far the best theorical model that describes interaction of this elementary particles. Is divided into two categories the bosonic sector and the fermionic sector. [2]
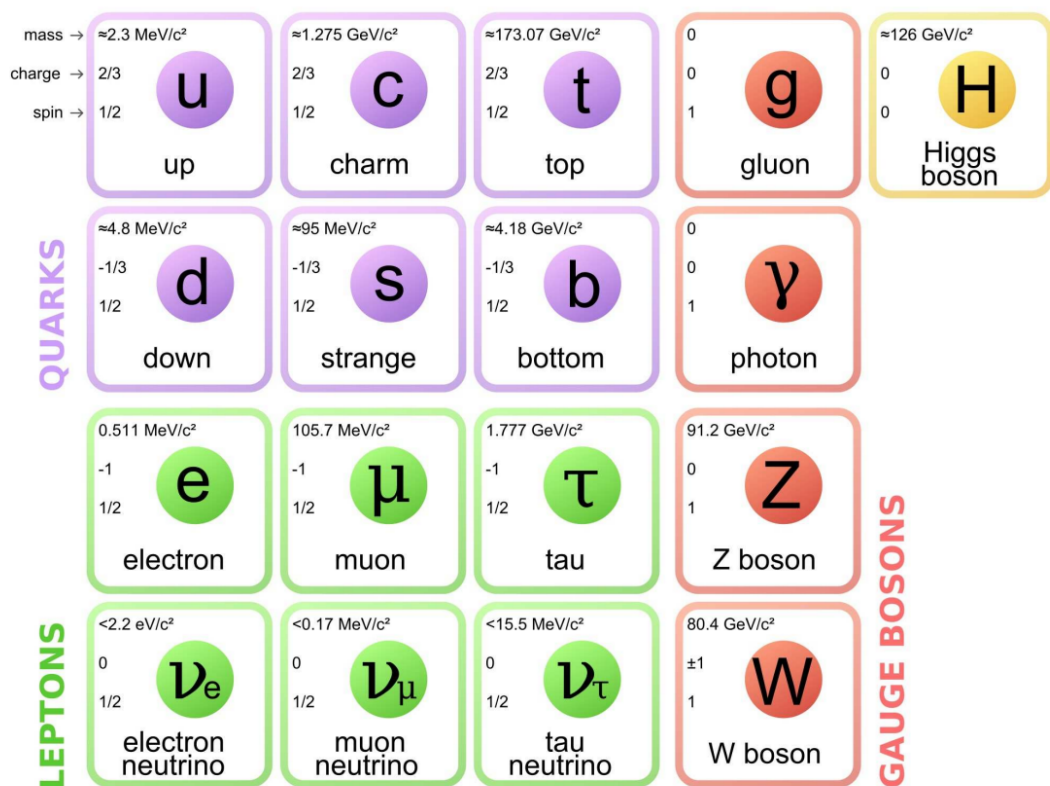
Fig. 1.2 The standard model of particle physics

The fermionic sector contains particle the particles that make up all known matter in the universe and is divided into the leptons and the quarks, both of this particles are divided into three generations, each generation being heavier than the one before. For the leptons we have electron and Its neutrino for the first generation, the second generation is. the μ and Its neutrino and the third one is the with Its neutrino. In the case of quarks we have the quark up and the quark down for the first generation, the second generation que have the quark charmd and the quark strange and for the third generation que have the quark top and the quark bottom. The bosons are the mediator particles called the gauge bosons

already mentions, the photon, the gluon, the bosons $W\pm$ and the boson Z. There is also de Higgs bosson, which is the last gauge bossons and It's the responsible to give mass to the other SM particles

One of the main sources to obtain elementary particles is particle accelerators, in this you accelerate a particle into high energy and smash them with a target, with the proper arrangements of magnets you can study the debris from the collision, for more heavy particles you need higher level of energy to the collision.

1.2   Large Hadron Collider

The Large Hadron Collider (LHC) is the biggest and powerful particle accelerator in the world at this moment, It is a 27 kilometers ring of superconducting magnets, this magnets boost the particles energies to obtain speeds that are close to the light speed before collisions. These particles are introduced as to the accelerator as particles beams this beams travel in opposing directions in tubes that are kept at ultrahigh vacuum, with the help of a electromagnetic field made by the electromagnets operating in superconduct state at low temperatures thanks to liquid helium this particles are guided across the whole accelerator. [3]

The LHC is part of an accelerator complex in CERN that is a succession of different machines that increase the energy of the beam of particles before passing into the next one on the sequence the particles at last are introduced on the LHC which is the last element in the sequence. The particles start at the linear accelerator 4 (Linac4) which is the source of the protons beams, it accelerates the particles in this case negative hydrogen ions to 160 MeV to enter the Proton Synchroton Booster (PSB), this is were the hydrogen loses Its two electrons leaving only protons and accelerating the beam to 2 GeV and then are injected into the Proton Synchroton (PS), in where the protons are accelerated up to 26 GeV and then they are sent into the Super Proton Synchroton (SPS) here they are accelerated up to 450 GeV and then they're finally introduced into two beams pipes on the LHC, it takes about 4 minutes and 20 seconds to fill the LHC rings reaching energies up to 6.5 TeV, there are 4 collisions points where the detectors are located Alice, Atlas, CMS and LHCb, in the collision the total energy is of 13.6 TeV. [4]

The LHC has been working since 2009 with the discovery of the Higgs Boson on 2012 and looking for new physics It has been working on different periods called Runs, Run 1 was on the period of (2009-2013), Run 2 was on (2015-2018), Run 3 is currently on going since 2022.
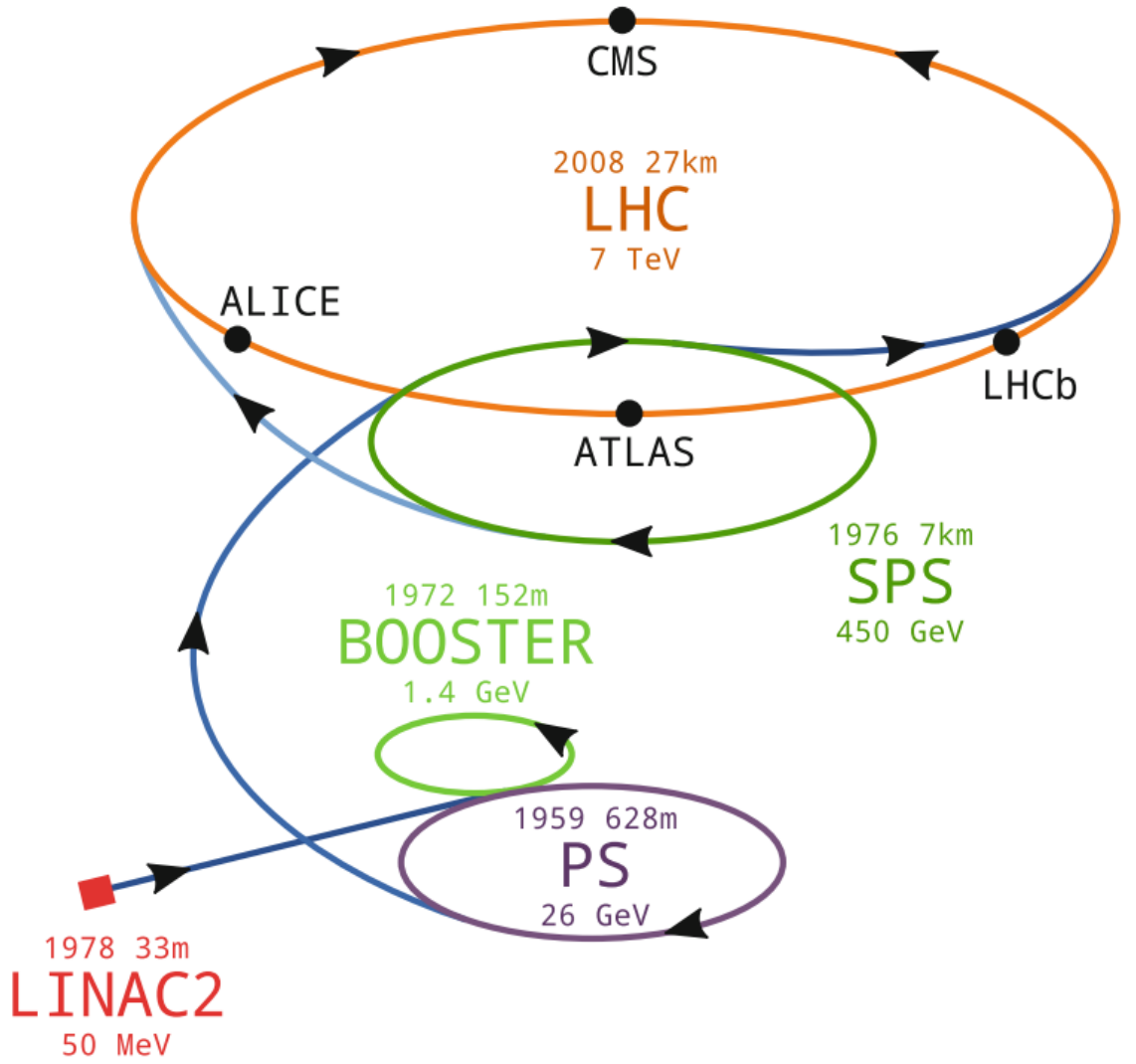
Fig. 1.3 The accelerator facility at cern for the LHC

1.3 Luminosity

The performance of a collider is determined by the beam energy and the luminosity, the luminosity is a key parameter in particle colliders is a quantity that measures the ability of a particle accelerator to produce a required number of interactions and is given by: [5]

$$\frac{dR}{dt} = \mathscr{L} \cdot \sigma_p \tag{1.1}$$

In which $\frac{dR}{dt}$ is the number of events per second, the $_p$ is the cross section and L the instantanious luminosity luminosity. The unity of $\mathscr{L}$ is $cm^{-2}s^{-1}$ a higher luminosity means greater probability that the particles will collide and produce the desired interactions,

luminosity can be increased then in two ways, packing more particles into the beams or focusing this beams more.

To compute the luminosity of two there is a few things that need to be taken in consideration. First the density distribution of each beam in the transverse and longitudinal plane, with the. two beams moving towards each other, the position and the time as the cross each other also need to be considered and calling the distance to the collision point s_0. In principle each of the distributions is different the overlap integral can be written as follow:
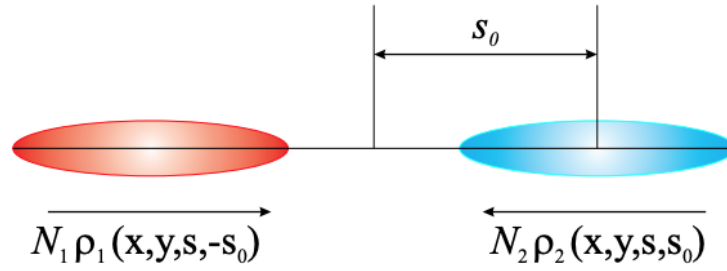

Fig. 1.4 Two beams colliding

$$2N_1N2fN_b \int \int \int_{-\infty}^{\infty} \rho_{1x}(x)\rho_{1y}(y)\rho_{1s}(s-s_0)\rho_{2x}(x)\rho_{2y}(y)\rho_{2s}(s+s_0)dxdydsds_0 \quad (1.2)$$

With N1 and N2 being the bunch intensity, f the revolution frecuency, N_b the number of colliding bunches, ρ_1 and ρ_2 time dependent beam density distribution functions, this is assuming the velocity on the beams is $v1 = -v2$ and the densities are uncorrelated in all planes the overlap integral takes the form of: [6]

For solving this integral one should known all distributions and an analytical solutions might not be possible and numerical numerical integration might be required.

The instantaneous luminosity is important but the final important number is called integrated luminosity. The integrated luminosity considers the total number of events during a data period is defined as:

$$L_{int} = \int L(t')dt' \quad (1.3)$$

it is related directly to the number of observed events

$$\mathscr{L}_{int} \cdot \sigma_p = number of events of interest \quad (1.4)$$

There have been different luminosities reached on the LHC for the Run 1 a luminosity of $0.77 x 10^{34}$ was reached and a integrated luminosity of 25 fb^{-1} with a precision of 2.0% for the first part and second part of the Run 2 the luminosity measured was of 38.4 fb^{-1} with a precision of 1.3% and $78 fb^{-1}$ respectively[7]. The following image show shows the integrated luminosity for the CMS experiment on different years.
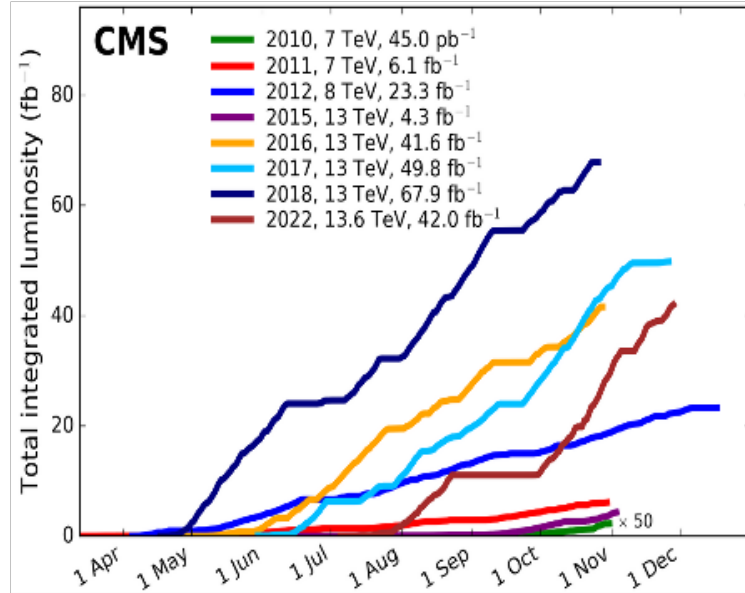

Fig. 1.5 Integrated luminosity at CMS

Chapter 2

CMS Experiment

2.1 CMS detector

The Compact Muon Solenoid (CMS) detector is one of the four interactions points on the LHC. It consist on different detectors made for different purposes, the silicon tracker, the electromagnetic calorimeter (ECAL), the hadron calorimeter (HCAL) the superconducting solenoid and the muon chamber.

The CMS has the form of a cylindrical onion with several concentric layers of components, this components are important to determine the properties of different particles all of this by bending their trajectories with a magnet that bend charged particles, this helps to identify the charges of the particles since they bend in different directions and allows to measure the momentum of a particle sine high momentum particles bend less than the low momentum ones. The principal magnet of the CMS is called Super Conducting Solenoid this magnet generates a field of about 4 Teslas and is very large 6.3m cold bore, 12.5 meters of length and 200 t of mass. The high magnetic field is confined to the volume of the detectors using the "return yoke", this yoke have a magnetic field strength of 2 Teslas and acts as the main support as well as the muon filter Its made of a high amount of steel and It weights more than 11000 tonnes. [8]

One of the principal objectives of the CMS is identify with very high precision the paths taken by the particles that were bend by the magnetic field they called this part the inner tracker which is composed of different substructures, closest to the interaction point we have the Silicon Pixel Detector, then after the silicon strip detectors which are divided into the inner barrel part and the outer barrel part, the outer barrel and the outer end caps. When a charged particle pass through this layers interacts electromagnetically with the sensors leaving a hit that can be used to identify the path that a particle took. [9]
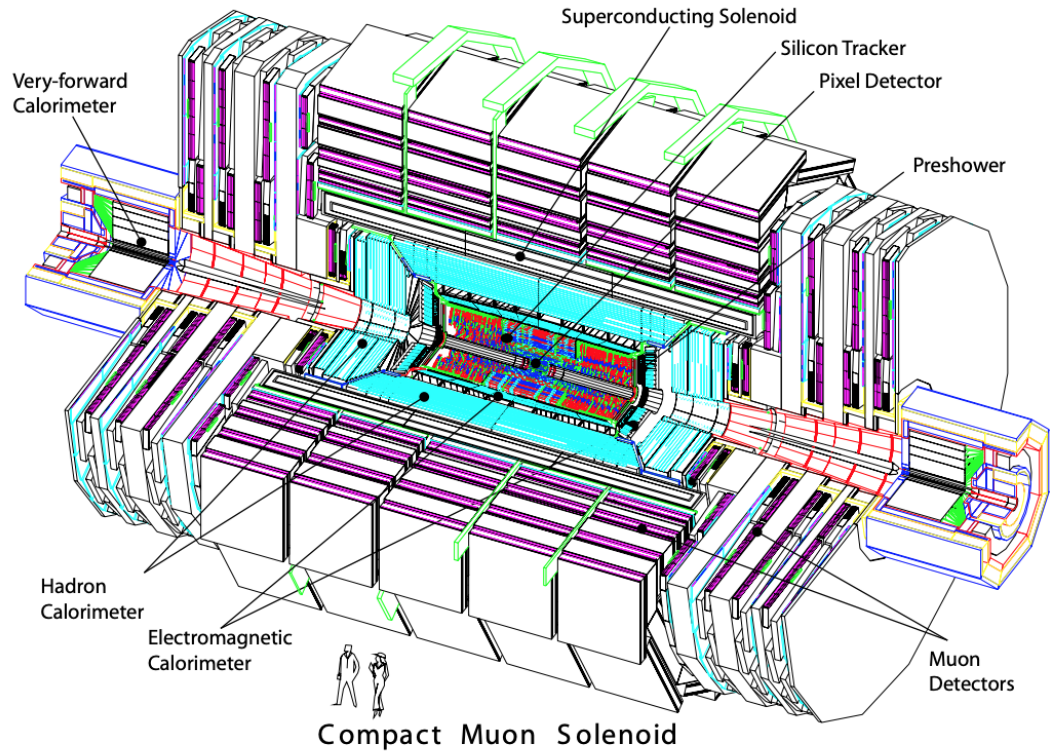
Fig. 2.1 The CMS detector size comparison with each of their components

Having information of the energy is important to understand what is happening at the collision point for this purpose there are two calorimeters on the CMS. The ECAL is made of 61200 lead tungstate crystals in the central barrel cap closed by 7324 crystals in the two of the endcaps in front of this crystals there is a press shower detector, the high density crystals allow the calorimeter to be fast, have a fine granularity and being radiation resistant, Its capabilities are improved by the good crystal resolution which are provided by a homogeneous crystal calorimeter. It's surrounding the tracker and aims to measure the the energy of electrons, positrons or photons and stop them completely. The other calorimeter is the HCAL which is surrounding the ECAL and plays an essential role on the measurements of the energy of hadrons like the quarks, gluons, neutrinos and some exotic particles. which are also stopped here.

The CMS was optimized for the detections of muons and is the last particle that the CMS observe directly with the help of the muon chambers that is composed by many subdetectors which are interleaved with the return of the yoke of the solenoid located after the super conducting solenoid, muons are similar to electrons but 200 times heavier so
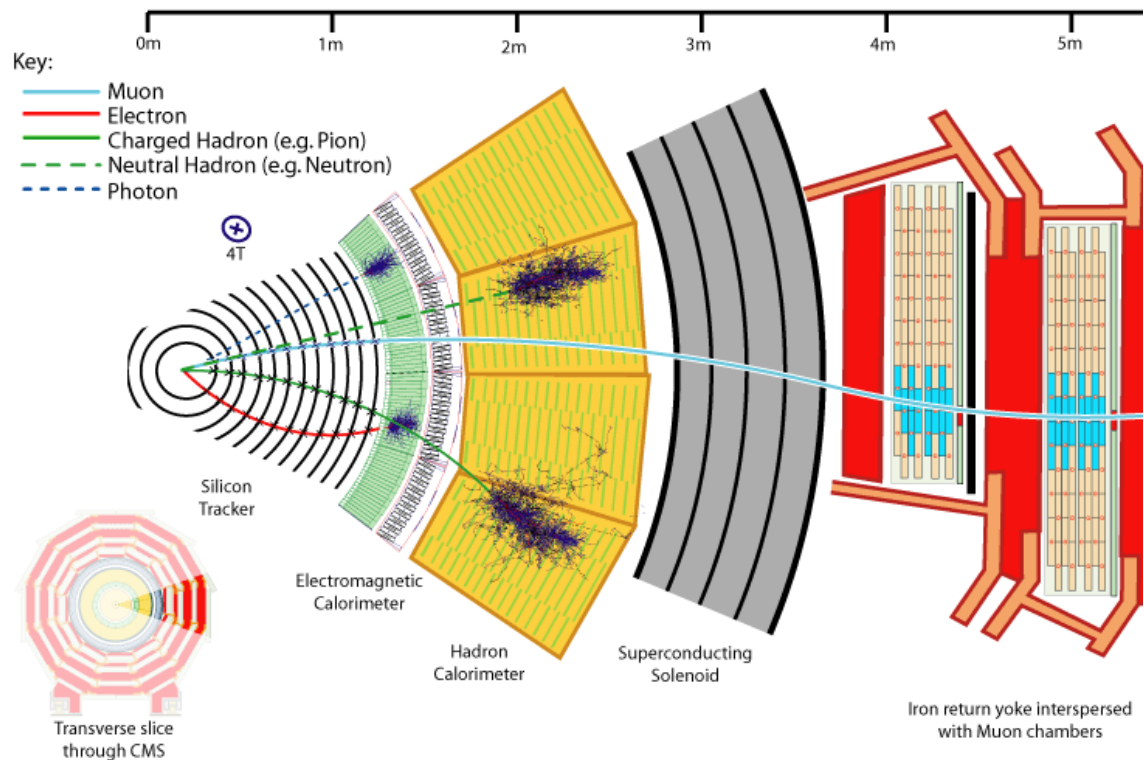
Fig. 2.2 Different particles travelling across the different detectors of the CMS experiment

they are not stopped by the calorimeters, the muon chambers have 3 main purposes; muon identification, momentum measurement and triggering. [10]

2.2   Pixel Detector

In the innermost part part of the CMS experiment there is a silicon pixel detector which is part of the tracking system. It has the task of provide high resolution 3D space points close to the collision point for track patter recognition and vertex reconstruction. It is located in a place where there is a harsh radiation environment giving Its high track density, in the CMS there was an pixel detector that was later changed during the first long shut down of the LHC during LS1 (2013-2014) and replaced by the CMS Phase-1 Pixel Detector in order to mantain efficient and robust tracking giving that with the upgrade of the accelerators the luminosity have doubled compared to the design value. It is expected that this detector to deliver high quality data until the end of the LHC Run 3 (Currently in process) after which the whole track detector on the CMS will be replaced.

Overall, is the closest detector to the beam pipe with cylindrical layers in the range of 3cm and 16cm at either end so It's vital to reconstruct the tracks of particles with very short live spans. It contains 124 millions pixels that allows to the tracking of the particles

emerging from the collision with a extreme accuracy. It has 4 layers, each one of these layers is composed of silicon modules that are splitted into tiny silicon sensors this is what is called the pixels. These pixels have a size of 100 μm -150 μm, when a charged particle pass through this pixels it gives the electrons on the silicon enough energy to be ejected with an applied voltage these charges are collected as a small signal which is amplified by an electronic readout ship. With these signals we can know which pixels were touched, allowing us to recreate the track using the 2D tiles detectors and with the help of Its 4 layers can also generate a 3D picture. Nevertheless, the rate of the particles passing through this detectors is big at 3cm to the beam pipe the rate is about 600 million of particles $^2/s$ the pixel detector is able to reconstruct all the tracks the particles leave behind. Each of the 124 million pixels are kept to a minimum power, even with only 50 microwatts per pixel the total power output of the whole detector is it about 7.5kW. It also has a freezing system of cooling tubes and kept about 20 degrees celsius reducing the damage to the modules made by the large stream of particles.

The layout of the detector is optimized to have four hit coverage over the pseudorapidity range of $|\eta| < 2.5$ which is important to improve the pattern recognition and track reconstruction and added redundancy to cope with hit loses. Apart from this the detector consist in the already mentioned four concentric barrel layers (L1-L4) with specific radius of 29mm, 68mm, 109 mm and 160 mm and three disks (D1-D3) on the ends with distances to the center of 291mm, 396mm and 516mm and the total silicon area is of 1.9 m^2. The detector is built from 1856 silicon sensor modules, 1184 of these are on the barrel pixel detectors (BPIX) and the rest one are on the forward pixel detectors (FPIX), each module consist in a sensor of 160x416 pixels connected to 16 readout chips (ROCs) for a total of 124 millions readout channels. [11]

The BPIX and FPIX detectors are independent components, the BPIX consist in two half barrels with a length of 540mm each of the four layers are called half shells and is divided into two mechanically independent halves both composed of one half detector and two service half-cylinders. The FPIX is assembled from twelve disks which are divided into inner and outer half rings which supports 22 and 34 modules respectively and is divided into four mechanically independent quadrants each formed by three half-disks installed in a service half cylinder. This detectors are supplied with four service half-cylinders that hold the readout and control circuits.

In order to optimize the resolution of the tracking and the vertexing the materials used in the detector were minimized. Even with the additional layers the material budget for the CMS Phase-1 Pixel in the central region is almost the same as the original detector while reducing the forward region. This is possible thanks to the advanced nano carbon-fiber materials for the mechanical structure that adopt the usage of lower mass, and two phases
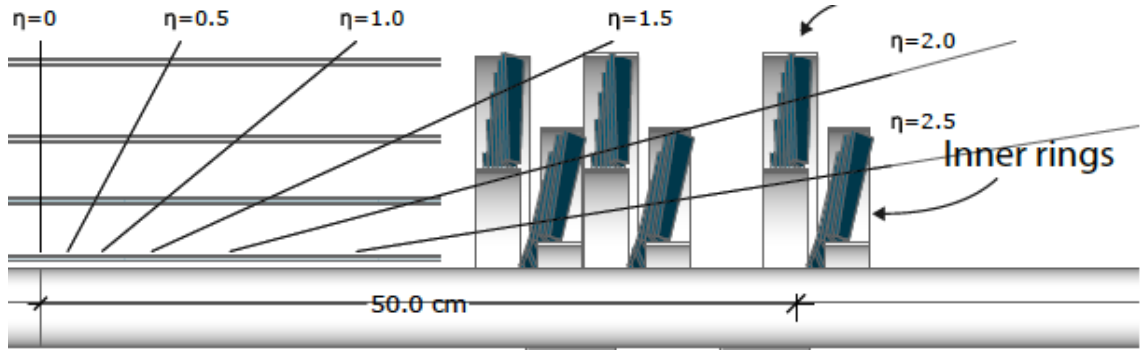
Fig. 2.3 Pixel detector outter rings and inner rings structure

CO_2 cooling systems. The electronics boards on the service half-cylinders are placed in higher pseudorapidity regions outside of the tracking acceptance.

The innermost layer have to support high levels of radiation and hit rates a hadron fluence of $3.6x10^{15}n_{eq}/cm^2$ (neq is the units of 1 MeV of neutrons equivalent) is expected in the innermost layer after collecting a integrated luminosity of 500 fb^{-1}. In the outer layers of the BPIX and on the FPIX the expected hit rates are of about $600MHz/cm^2$ for BPIX L1.

The silicon detector modules is built from a planar silicon sensor bonded to an array of 2x8 ROCs. Each ROC is segmented on 4160 readout channels and reads information about each pixel. Since 2 ROCs can only be placed at a minimum distance between each other pixels along the ROC boundaries have twice the area and those at the corners have four times the area of a pixel, in the other side of the silicon sensor there is a high density interconnect (HDI). To simplify the module production as well Its maintenance, the same rectangular module geometry is used for both BPIX and FPIX detectors. In the BPIX detector the orientation of the sensor surface is parallel to the magnetic field, this means that the pixels are oriented parallel to the beam line. The FPIX detectors in the outer rings are rotated 20 degrees, in the inner ring the modules are arranged in an inverted cone array with an angle of 12 degrees respect to the beam line combined with the 20 degrees rotation. The orientation for the FPIX is made such as the long side of the pixels is in the radial direction.

The sensors of BPIX and FPIX were designed by two different companies, BPIX was made by CiS Forschungsinstitut fur Mikrosensorik in efurt on germany and FPIX was made on SINTEF micro-systems and sensors in Norway. The BPIX sensors were made on approximately 285 μm of phosphorous-dope 4-inch wafers from silicon mono-crystals, all of this sensors were produced using silicon from the same ingot. In the other side, the FPIX sensors were made on 300 μm thick 6 inch float-zone wafers, eight sensors were placed on one wafer, the wafers were accepted if at least six of It's sensors fulfill their specifications.
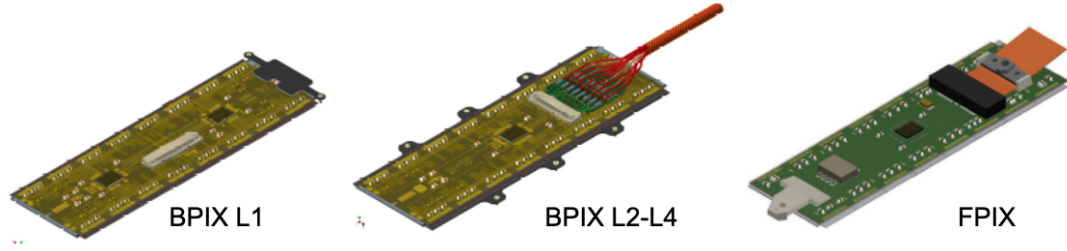
Fig. 2.4 Barrel Pixel Detector moudles and Forward Pixel Detector Modules

The readout chips are made using 250 nm CMOS technology, this are named PSI46dig and PROC600. The PSI46dig is used on the outer BPIX layers (L2-L4) and in the FPIX detectors, meanwhile the PROC600 was designed for the innermost layer, taking into the consideration the expected hight hit rates. The single pixel efficiency of the PSI46dig at high rates was measured using internal calibration signal while exposing the ROCS to high-rate X-rays, the data loses for both of the detectors were of less thant 2 % at the expected maximum hit rate of 120 MHz/cm^2 and the PROC600 efficiency is above 95 % at rates up to 600 Mhz MHz/cm^2.

2.3   Pixel Cluster Counting

The Pixel Cluster Counting (PCC) method consist in counting the average number of pixel clusters on the detector to measure luminosity. This occurs during a zero bias event, an event that is trigged by requiring only that two proton bunches cross at the CMS interaction point. Giving that the number of pixels in really big the probability that a pixel is being hit by two different tracks by the same bunch crossing is really small. The mean number of pixel clusters in a simulated zero bias event is in the order of 100 per pp collision. The number of pixel clusters per bunch crossing is linearly dependent on pileup and therefore an accurate measure of the instantaneous luminosity.[12] The mean number of pixel cluster per trigger is

$$< N_{cluster} >=< N_{Pixel/Interaction} >< N_{interaction} >=< N_{Pixel/interaction} > \mu \qquad (2.1)$$

here the μ is the number of interactions and with this the following equation and gives us a relation with the cross section $_i$, instant luminosity and μ

$$\mu = \frac{\sigma_i}{f}\frac{dL}{dt} \tag{2.2}$$

here f is the frequency of the LHC, defining a new quantity $_{cluster} = _i < N_{Pixel/Interaction} >$ and combining equation (2.1) and (2.2) we got

$$< N_{cluster} >= \frac{\sigma_{cluster}}{f}\frac{dL}{dt} \tag{2.3}$$

Here, the value of $N_{cluster}$ is the mean number of pixel clusters on the pixel detector during a zero bias trigger at a head on period, the value of $\sigma_{cluster}$ can be obtained using the Van Der Meer scan and from the equation (2.3) we can obtain the luminosity from [13]

$$\sigma_{cluster} =< N_{cluster} > f(\frac{dL}{dt})^{-1} \tag{2.4}$$

2.4   Pixel Detector Module Selection

To be applicable to a van der mer scan the cluster cross section must use exactly the same detector configuration during the whole of the data taking and the calibration scan. This means if any of the modules of the detector didn't work at any point of the scans and didn't gave any readout It must be excluded from the calibration and the luminosity analysis, the stability of each module is determined in a ratio of module PCC and total PCC. [14]

From the total of 1856 modules on the pixel detector (1184 on the BPIX and 672 on FPIX) so in the analysis for the pcc vdm calibration onf 2024 for the fill 9639a total of 240 modules were used.

Chapter 3

Luminometer Calibration

3.1 Van Der Meer Method

The Van Der Meer (vdM) scan let us obtain the value of $\sigma_{visible}$ using different luminometers. For this case the detector of interest is the pixel detector with which are going to obtain a calibration of the luminosity using the vdM scan in combination with the PCC method. The scan consist on separating particle the beams from each other between the X and Y axis by ΔX and ΔY values moving them and recording values of luminosity independently, when the scan on X and scan on Y are imposed over each other we said that they're on head on giving the maximum value of luminosity. Usually a single gaussian fit is used to obtain beam overlap widths also denoted as Σ_x and Σ_y, other fit models may be used like the doble gaussian depending on the quality of the fit [15]
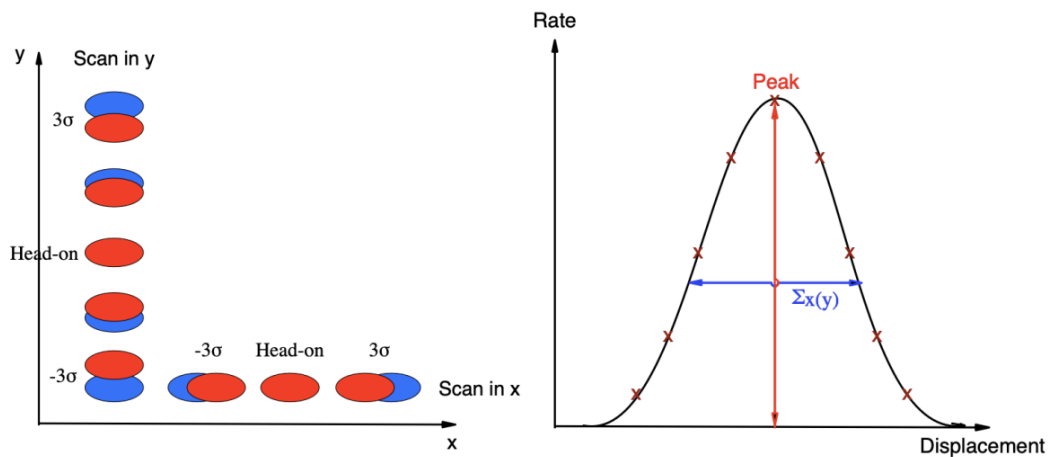

Fig. 3.1 The vdm scan on the left showing the beams for X and Y. On the right a curve of the different values of rate for the beams displacement, the peak occurs during the head on part.

For obtaining the importnat parameters on the vdm scan we return to the equation (1.2) and apply it to and individual bunch crossing, the values of N1 and N2 being the number of protons colliding can be obtained since is a known quantity from the experiment, the frequency f is also a known quantity, the frequency of the LHC which is 11,245 kHz but the proton densities ρ_1 and $\rho2$ are more difficult to obtain, this is were the vdM scan help us to measure integral over the bunch proton densities. The luminosity integral evaluated with the beams separated by a distance Δ_x and Δ_y can take the form of:

$$L(\Delta x, \Delta Y) = N_1 N_2 f \int \int \rho_1(x,y)\rho_2(x+\Delta x, y+\Delta y)dxdy \tag{3.1}$$

Because of the scan method is it assumed that the two bunches of proton densities are factorizable since they act independently between each other so we can turn the right part of (3.1) into two integrals:

$$N_1 N_2 f \int \int \rho_1(x,y)\rho_2(x+\Delta x, y+\Delta y)dxdy = N_1 N_2 f(\int \rho_1(x)\rho_2(x+\Delta x)dx)(\int rho_1(y)\rho_2(y+\Delta y)dy)$$
$$\tag{3.2}$$

Integrating both sides on Δy and using in combination with (3.1) while we fix $\Delta x_0 = 0$ and $\Delta y_0 = 0$ as the head on point, we obtain:

$$N_1 N_2 f \int \rho_1(x)\rho_2(x+\Delta x_0)dx = \int L(\Delta x_0, d\Delta y)d(\Delta y) \tag{3.3}$$

A similar result is obtained when we integrate both sides for Δx using this and combining equation (3.1), (3.2) and (3.3) we can obtain that

$$N_1 N_2 f \int \rho_1(x)\rho_2(x+\Delta x_0)dx = \frac{L(\Delta X_0, Deltay_0)}{\int L(\Delta x_0, \Delta y)d(\Delta y)} \tag{3.4}$$

Similarly to the previous step we can obtain the value of the other factor of (3.2) with an analogous process. The integrals resulting on the right side can be evaluated by evaluated by obtaining the rate in function of the beam-beam separation which are Δx and Δy this because the luminosity has a linear relationship with the rate. The Luminosity can be expresed on terms of the rate during the head on points using the following:

$$L(\Delta x, \Delta y) = N_1 N_2 f \frac{2R(\Delta x_0, \Delta y_0}{\int L(\Delta x_0, \Delta y)d(\Delta y) \int L(\Delta x, \Delta y_0)d(\Delta x)} \tag{3.5}$$

Here the luminosity is replaced by the rate R, it is convenient to write this integral in terms of the convoluted beam widths which are denoted by Σ_x and Σ_Y, this convoluted widths are defined by:

$$\Sigma_x = \frac{1}{2\pi} \frac{\int R(\Delta x, \Delta y_0 d(\Delta x))}{R(\Delta x_0, \Delta y_0)} \tag{3.6}$$

For Σ_y the result is analogous. With (3.6) we can write (3.5) in a different manner:

$$L(\Delta x, \Delta y) = \frac{N_1 N_2 f}{2\pi \Sigma_x \Sigma_y} \tag{3.7}$$

This in combination with (1.4) make us possible to obtain the following expression for the visible cross section

$$\sigma_{vis} = \frac{2\pi \Sigma_x Sigma_y R(\Delta x_0 \Delta y_0)}{N_1 N_2 f} \tag{3.8}$$

This makes possible obtain σ_{vis} only by experiment since all of the right values can be obtained via the experiment, the maximum rate $R(\Delta x_0, \Delta y_0)$ is obtained at the maximum PCC obtained during the vdm scan, this means during the head-on process.

3.2 Datasets

3.3 Scans

3.4 Background Estimation

3.5 Corrections

3.6 Fit model

3.7 Beam Parameters

The calibration constant

$$\sigma_{vis} =$$

$$L_b = \frac{2\pi \Sigma_x \Sigma_y R(0,0)}{N_1 N_2 f} \quad [6]$$

Chapter 4

Results

4.1 Sigma$_V$ is

4.2 Systematics

References

[1] David Griffiths. *Introduction to elementary particles*. Wiley-VCH, 2010. ISBN 978-3-527-40601-2.

[2] Mark Thomson. *Modern Particle Physics*. Cambridge University Press, 2013. ISBN 978-1-107-03426-6.

[3] A.B. Arbuzov. Quantum field theory and the electroweak standard model. 2018.

[4] Esma Mobs. The cern accelerator complex. July 2019.

[5] Bruno Muratori Wener Herr. Concept of luminosity. *CAS - CERN Accelerator School: Intermediate Accelerator Physics*, pages 361–378, 2006. doi: 10.5170/ CERN-2006-002.361.

[6] Simon White. *Determination of the absolute luminosity at the LHC*. Phd thesis, University of Paris SUD 11, October 2010.

[7] The CMS collaboration. Precision luminosity measurement in proton-proton collisions at 13.6tev in 2022 at cms. March 2024.

[8] Dave Barney. An overview of the cms experiment for cern guides. 2003.

[9] The CMS collaboration et al. The cms experiment at the cern lhc. *Jinst*, 2008.

[10] S. Chatrchyan. The cms silicon strip tracker. *Journal of physics conference Series 41*, 2006. doi: 10.1088/1742-6596/41/1/011.

[11] CMS Tracker Group of the CMS collaboration. The cms phaces-1 pixel detector upgrade. *JINST 16 (2021) P02027*, 2022. doi: 10.1088/1748-0221/16/02/P02027.

[12] The CMS collaboration. Cms luminosity based on pixel cluster counting -summer 2012 update. March 2018.

[13] The CMS collaboration. Luminosity measurement at cms. March 2018.

[14] The CMS collaboration. Precision luminosity measurement in proton-protoncollisions at s = 13 tev in 2015 and 2016 at cms. March 2018.

[15] Yusuf Can. *Calibration of CMS luminometer using Van Der Meer and Emittance scans*. Phd thesis, Bogazici University, October 2018.